WARSAW UNIVERSITY OF TECHNOLOGY Index 351733
FACULTY OF CIVIL ENGINEERING
COMMITTEE FOR CIVIL AND WATER ENGINEERING
POLISH ACADEMY OF SCIENCES ISSN 1230-2945

DOI: 10.24425/ace.2021.138063

ARCHIVES OF CIVIL ENGINEERING

Vol. LXVII ISSUE 3 2021

s. 415–435

Research paper

Experimental investigation into material characteristics of pea gravel

J.L. Zhang[1], Q.X. Huang[2], Ch. Hu[3], Zh.Q. Wang[4]

Abstract: Pea gravel is a kind of a coarse aggregate with a specific particle size used to fill the annular gap between the lining segments and the surrounding ground when tunnel construction with shield machines is performed in hard rock. The main purpose of the present study is to propose quantitative morphological indices of the pea gravel and to establish their relations with the void content of the aggregate and the compressive strength of the mixture of pea gravel and slurry (MPS). Results indicate that the pea gravel of the crushed rock generally have a larger void content than that of the river pebble, and the grain size has the highest influence on the void ratio. Elongation, roughness and angularity have moderate influences on the void ratio. The content of the oversize or undersize particles in the sample affects the void ratio of the granular assembly in a contrary way. The compressive strength of the MPS made with the river pebble is obviously smaller than that of the MPS made with the crushed rock. In the crushed rock samples, the compressive strength increases with the increase of the oversize particle content. The relations between the morphological properties and the void content, and the morphological properties and the compressive strength of the MPS are expressed as regression functions. The outcomes of this study would assist with quality assessments in TBM engineering for the selection of the pea gravel material and the prediction of the compressive strength of the MPS.

Keywords: pea gravel, morphological properties, uncompacted void content, compressive strength, digital image processing, shield TBM

[1] Prof., PhD., Eng., Yellow River Engineering Consulting Co.,Ltd. Zhengzhou, Henan, China, e-mail: jlzhangyrec@126.com

[2] Prof., PhD., State Key Lab of Geohazard Preventionand Environment Protection (SKLGP), Chengdu University of Technology (CDUT),Chengdu, Sichuan, China, e-mail: qiuxiang.huang@foxmail.com, ORCID: https://orcid.org/0000-0002-5541-6009

[3] Master, State Key Lab of Geohazard Preventionand Environment Protection (SKLGP), Chengdu University of Technology (CDUT), Chengdu, Sichuan, China, e-mail:1299158914@qq.com

[4] Eng., Yellow River Engineering Consulting Co., Ltd. Zhengzhou, Henan, China, e-mail: djhbsy@126.com

1. Introduction

When tunnel construction is performed with shield machines, a gap remains behind the shield tail between the lining segments and the surrounding ground termed the annular gap. This gap has to be filled with a suitable material in order to provide appropriate bedding for the segment tube and to ensure a uniformly distributed transfer of the loading from the ground pressure and also to counter any loosening of the surrounding ground [1–2].

The quality of this fill material (termed as backfill) is of significant importance for the stability of the lining. The used material affects the interaction between the support and rock mass. Therefore, the choice of a proper backfilling material is of great importance for the system behavior [3–5].

In the case of shielded hard rock tunnel construction with boring machines the annular gap is filled with pea gravel [4]. The grain size distributions between 4 and 16 mm are generally applicable. In order to avoid blockages within the annular gap, the percentage of the undersized grains should be kept below 10%. Also, the gravel should have no fines in order to minimize clogging [6–7]. The pores in the gravel fill can then be grouted with fluid mortar in a subsequent working stage. It is required that the “annulus” must be uniformly filled completely. Generally, it is considered that the larger the void content in the pea gravel accumulation, the larger the filling rate of the slurry in the backfill grouting, which means a better grouting quality and better workability of the mix.

According to the above engineering background, from the material point of view, the pea gravel material is a kind of a coarse aggregate with a specific particle size, while the mixture of pea gravel and slurry (MPS) is a special kind of a concrete. The aggregate is composed of the individual material particles. The material properties of the individual particles play an important role in the engineering effect of coarse aggregates. The characteristics of the individual particles (such as parent rock type, particle shape, particle size, angularity and surface roughness) can affect the bulk properties of the granular assembly (including the particle size distribution, void ratio, etc.), and can have important impacts on the performance of the mixture [8–14].

Many useful results have been obtained from previous research. Particle shape and size have been considered as the most important factors affecting the gravel aggregate’s properties. Kawamoto et al. [15] carried out research to study the effect of aggregate properties on particle rotations and stress via a mechanics-based 3-D particle shape index. Wu et al. [16] conducted research to characterize the three-dimensional shape of aggregate and provided an accurate aggregate model for finite element numerical simulation. Nikbin et al. [17] investigated the effects of different variables (i.e. maximum coarse aggregate size, coarse aggregate volume and aging) on the mechanical behavior of

self-compacting concrete. Specimens prepared using the super pave gyratory compactor with different aggregate sizes have noticed different air void sizes, as reported by Masad et al. [18]. In the research conducted by Meddah et al. [19], four granular fractions were combined in different proportions to investigate the effect of the particle size distribution of aggregate on the properties of concrete. Also, the influence from the surface texture has been investigated in reported results [20–22]. However, few studies have been done focusing on the morphological properties of pea gravel, and its effects on the bulk property of void content, as well as on the relation with the compressive strength of the MPS.

As a particulate composite material, the physical and mechanical properties of the MPS are strongly influenced by its constituent materials. The aggregate typically occupies more than half of the volume of the mix and plays an important role in determining the physical properties and mechanical behavior. In addition, according to the results of the conducted studies mentioned above, the morphological characteristics of the individual particles have an important influence on the construction of the aggregate space skeleton, resulting in significantly influencing the behavior of the mixture. In this context, establishing the relation between the morphological characteristics and the void content of the pea gravel aggregate and the compressive strength of the MPS is of great significance in engineering aspect for the selection of the pea gravel material, the quality assessment of the backfill and the prediction of the MPS strength.

The main purpose of the present study is therefore to propose the quantitative morphological indices of the pea gravel and establish their relations with the void content of the aggregate and the compressive strength of the MPS. For this purpose, three types of experiments were carried out on 10 pea gravel samples to obtain the morphological indices, the void content and the compressive strength, respectively. Then the data were systematically analyzed to investigate the correlation of various morphological properties to the uncompacted void content and to the compressive strength of the MPS. In addition, the relations are expressed as functions using regression analysis, which can assist with quality assessments in engineering.

However, the compressive strength of the MPS is not only affected by the type of the pea gravel but also by the slurry and the construction procedure. The interactions that occur at the interface between the aggregate particles and the cement paste which surrounds and binds them may influence many of the properties of the MPS. In the present study, focused on the influence of the aggregate only is done without taking into account the effect of the slurry. A common slurry is used to mix with different pea gravel samples.

2. Material and methods

2.1. Materials and specimens

There are two kinds of pea gravel materials used in engineering: (a) artificial gravel (crushed rock) and (b) natural gravel (river pebble). In China, the grain size range of the pea gravel is 5–10 mm, and the oversize and undersize contents have limitations.

In this study, 4 pea gravel material were collected from 4 different places, considered as original pea gravel material, numbered S1–S4 (see in Fig.1), respectively. Among them, S1–S3 is artificial gravel, sampled from TBM construction projects, and S4 is natural gravel. The basic information of the 4 original pea gravel material is shown in Table 1 and Fig.2. The oversize content is the weight percent of particles with the size over 10 mm, while the undersize content is the weight percent of particles with the size under 5 mm.

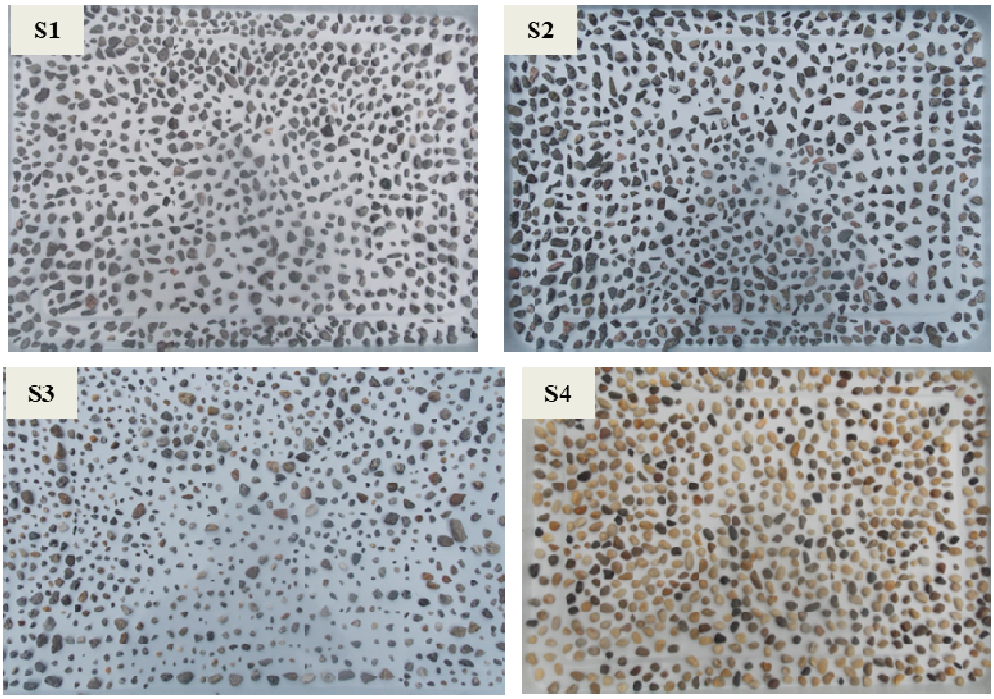

Fig. 1. Photos show the particle morphology of the four initial pea gravel material

Table 1. Properties of obtained original pea gravel materials

ID	S1	S2	S3	S4
Type	Crushed rock	Crushed rock	Crushed rock	River pebble
Oversize content (%)	8.48	15.61	4.47	0.01
Undersize content (%)	3.98	5.01	15.28	0.007

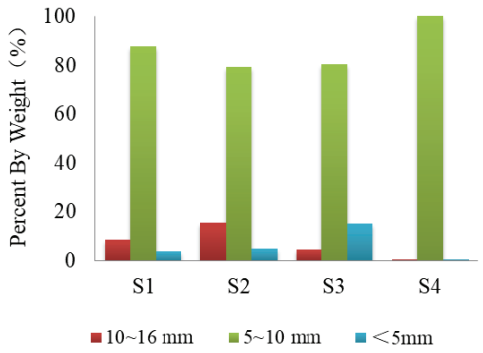

Fig. 2. Sieving results of the 4 original pea gravel materials

To investigate the effect of the content of the oversize and undersize particles, 5 mixed pea gravel material (S5–S9) were made using S1 as follows: S5 with all particles sized 5–10 mm; S6–S8, no oversize and with undersize percentages of 2%, 5%, 7.5%, respectively; S9 with 2% oversize and 5% undersize. In addition, to consider the effect of the grain size, a specimen of large particle size (8–12 mm) was prepared using the river pebble, marked as S10.

The reason for the difference in the loose bulk porosity of the different pea gravel samples is due to the differences in the particle shape characteristics, the grain size, and the content of the oversize and undersize particles in each sample. The combined effect of these factors leads to a difference in the compressive strength of the MPS. Therefore, according to the above factors, the relation between the morphological characteristics, void ratio of the pea gravel and the compressive strength of the MPS will be experimentally analyzed based on the 10 pea gravel materials described above.

2.2. The uncompacted void content test

After the pea gravel is blown into the annular gap, it gets deposited freely under gravity in the ring space in an uncompacted condition without being subjected to any external force during the field construction process. Therefore, a test was carried out to obtain the uncompacted void content under a condition similar to the field situation. The test principle is to let the pea gravel freely stacked in a container in a loose condition with lateral restraint and then to measure its void content. The details of the test procedure are given below.

First, take a pea gravel sample of 1000 g and add distilled water to make it fully absorbed. After 24 hours, wipe the sample to a surface saturated state with a squeezed wet towel and then pour the sample freely under gravity into a measuring cup from a height of 10 cm and smooth the surface of the deposit (Fig. 3a). Then read the volume of the pea gravel (v) by the gradations on the container and measure the weight of the sample and the container (m_1). Next, place a test filter paper on the sample

surface and let the filter paper cover the sample surface as much as possible (see Fig. 3b). Then add distilled water to the measuring cup through the gap (Fig. 3c) until the surface of the filter paper is wet (Fig. 3d). Weigh the total mass (m_2) of the measuring cup, the sample and the water at this time.
Finally, the void ratio (V_C) of the pea gravel sample is calculated by the following equation:

$$V_c = \frac{m_2 - m_1}{d_w \times v} \times 100\% \tag{1.1}$$

where d_w is the density of water.

Following this test procedure, three void content tests were performed in parallel on each pea gravel material, and the average of the three results was taken as the void content value of the pea gravel sample.

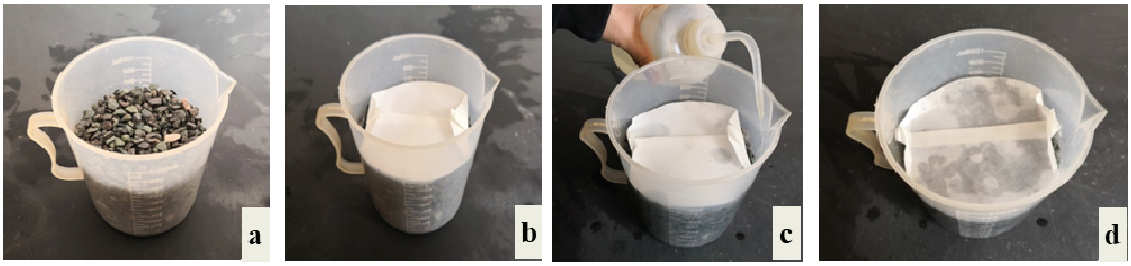

Fig. 3. Typical photos in the process of estimating the uncompacted void content

2.3. Imaging based morphological properties of the pea gravel

With the continuous development and improvement of digital image technology, the use of the digital image processing technology to quantitatively characterize the shape parameters of granular materials has become a hot topic. It has been successfully used in recent years [23–27]. In the present study, image analysis techniques were used to quickly obtain morphological characteristics of the pea gravel. This process involves four steps as stated below.
Firstly, a two-dimensional image was performed using a scanning device. The scanning type was a flat plate type, and the optical scanning resolution was 1200×1200 dpi. Before scanning, the pea gravel was placed one by one to ensure that the scanned image is the surface of the largest projection area and to prevent small particles overlapping each other to form large particles. Fig. 4a is the scanned original image.

It can be clearly seen that the pea gravel particles are not much different from the background color, making the edges of the particles not clearly distinguishable. Therefore, the next step was to convert the scanned image into a binary one (Fig. 4b, processed by Photoshop).

In the 3rd step, the obtained binary image was imported into the software Image-Pro Plus to measure the basic parameters including the shape, area, perimeter, diameter and contour data. After completing the measurement, the outline of the target particles was displayed on the working interface, and the particles were numbered and sorted from top to bottom, as shown in Fig. 4c and Fig. 4d.

Finally, the required particle morphological indices were calculated based on the obtained basic parameter information by mathematical processing.

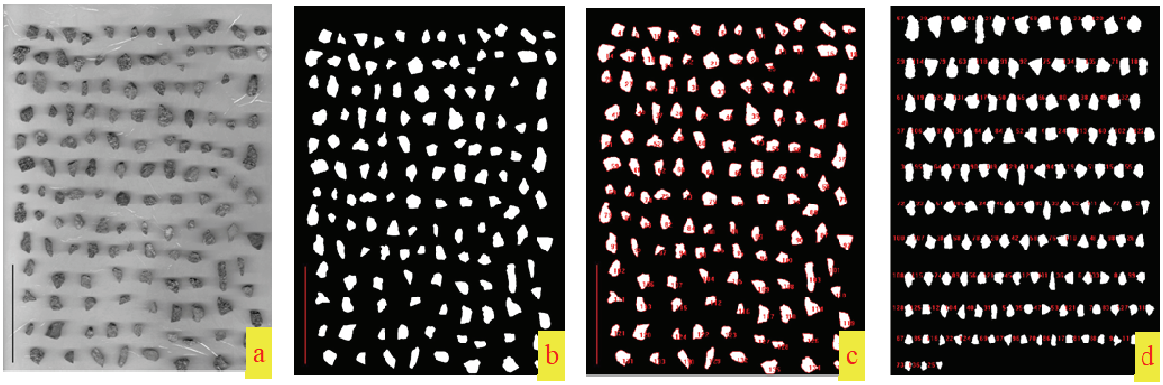

Fig. 4. Pea gravel image processing: a) original image, b) 2D binary image, c) pebble contours with identification numbers, d) reordered by area values

The morphology of the coarse aggregates includes the shape, size and surface texture. Many studies have been carried out on morphological indices with respect to evaluating them [28–34]. In the present study, the grain size of the particles is 5–10 mm, within a very narrow size range, so that the pea gravel is a kind of a single-sized aggregate. According to the characteristics of this kind of a material, the particle morphological indices were calculated considering the shape, size, and surface texture (see Table 2).

To obtain a mean value of a morphological parameter for the aggregate sample, an index value was established by averaging the index values of its particles weighted by their areas, as shown in the following equation:

$$Index = \frac{\sum_{i=1}^{n}(A_i \times Index_i)}{\sum_{i=1}^{n} A_i} \tag{2.1}$$

where: *Index* refers to each of the Indices in Table 2, respectively, $Index_i$ is the characteristics index of the i^{th} particle and n is the number of particles in the sample.

Table 2. Indices of the size, shape and surface texture used in this study [22, 24, 33–34]

Index denomination	Abbreviation and calculation formula of the index
Particle size	Length（L），width（W），particle area (A), particle perimeter (P)
Elongation, E	$E = L/W$ where, L is the length of the particle and W is the width of the particle.
Roundness, *Round*	$Round = \frac{P^2}{4 \times \pi \times A}$ where, P is the perimeter of the particle and A is the area of the particle.
Convexity Ratio，*CR*	$CR = \sqrt{\frac{A_c}{A}}$ where, A is the area of the particle and A_c is the area of the convex outline.
Angularity Parameter, *AP*	$AP = \left(\frac{P_c}{P_e}\right)^2$ where, P_c is the perimeter of the convex outline and P_e is the perimeter of the best approximating ellipse.
Roughness, *Rough*	$Rough = \left(\frac{P}{P_c}\right)^2$ were, P is the perimeter of the particle and P_c is the perimeter of the convex outline

2.4. Experiment of the compressive strength of the MPS

To visually simulate the process of mixing the pea gravel with the slurry in the annular gap, the present study produced a completely sealed cubic box (section size 26×26 mm), with two sides made of tempered glass (Fig. 5a). Considering making enough specimens for compressive strength test, each MPS model was designed with a height around 40 mm. The materials used in the experiment are the above described 10 kinds of pea gravel materials, and in all of those, the #425 cement was used to prepare the slurry with a w/c ratio of 0.6. The test steps are briefly described below.

Firstly, the pea gravel was poured into the model box, and then the configured slurry was poured from the bottom of the model box by pressure until the slurry covers the surface of the pea gravel. All the mixtures were kept in the model box for the first 24 h. After demolding at one day, the mixtures were continuously cured until the age of testing.

Secondly, for each mixture, six standard cylinder specimens were made for compressive strength test at 28 days, with the specimen dimensions of height (H) = 100 mm and diameter (D) = 50 mm, corresponding to an acceptable H/D ratio of 2:1, as shown in Fig. 5c.

Finally, the specimens were loaded in uniaxial compression using standard procedures for cylinder testing in a computer controlled automatic pressure testing machine. The average values of the results of the experiments for each MPS are presented in section 3.3.

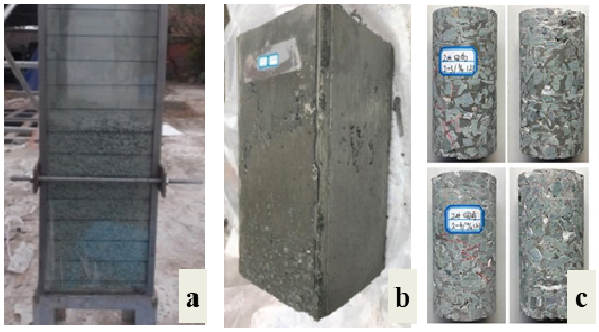

Fig. 5. Typical photos in the process of obtaining compressive strength: a) the completely sealed cubic box adopted to simulate the process of mixing the pea gravel with the slurry in the annular gap, b) the cured mixture, c) standard cylinder specimens for compressive strength test

3. Experimental results and discussion

3.1. Uncompacted void content

The uncompacted void content test results show that the void contents of tested samples range from 35.25 to 48.97. The experimental data parameters are not always consistent and show a wide variability. Test conducted by Ding et al. [35] showed that void content valued from 39.55 to 40.70. Value of which is close to the same aggregate size sample in the present study.

In loose condition, the angular and rough-textured aggregates generally have a larger void content than the rounded and smooth-surfaced aggregates. The lowest void content was found for S4, followed by the value for S10, both samples were river pebble.

Comparing the test results of the two river pebble samples shows that the grain size has slight influence on the uncompacted void content. The roughness and angularity have remarkable influence as compared to the grain size. Both S4 and S5 are in the range of 5–10 mm in diameter, and no oversize and undersize contents. It can be seen that the void ratio of the crushed rock sample (S5) is significantly larger than that of the river pebble sample (S4). Similar findings were also shown by Janoo et al. [36] that the volume of void in the aggregates was found to increase with increasing aggregate angularity.

The content of the oversize or undersize particles in the sample also affects the void ratio of the granular assembly. The samples S2, S7, and S9 are with the same undersize content of 5%, and it can be seen from the results that the void ratio increases as the oversize content increases. According to the comparison among the measurement results of samples S5 and S8, it is possible to say that the void ratio decreases as the % of undersize particles increases (see Table 3).

Table 3. Summary of the void content test results for the 10 pea gravel aggregates

ID	V_c (%)	Sample Description
S1	46.84	Original pea gravel, crushed rock
S2	48.97	Original pea gravel, crushed rock
S3	41.41	Original pea gravel, crushed rock
S4	35.25	Original pea gravel, river pebble
S5	42.36	Mixed pea gravel with oversize 0%; undersize 0%
S6	40.08	Mixed pea gravel with oversize 0%; undersize 2%
S7	39.59	Mixed pea gravel with oversize 0%; undersize 5%
S8	39.40	Mixed pea gravel with oversize 0%; undersize 7.5%
S9	43.91	Mixed pea gravel with oversize 2%; undersize 5%
S10	35.56	River pebble sizing 8–12 mm

3.2. Morphological characteristics

Through the observation of pea gravel samples, a qualitative understanding of the morphological characteristics of the pea gravel can be obtained easily. From the shape of the particles, it is easy to distinguish between the crushed rocks (angular shaped particles) and river pebbles (rounded shaped particles). According to the sieving results, it can be clearly seen that the particle size distribution of the natural pebble is uniform, and there are more large particles in S2 and more small particles in S3. But this information cannot help us quantify the contribution of the morphological characteristics of particles to the activity of granular assembly. Therefore, it is necessary to quantify the morphological characteristics.

Image analysis techniques were used to quickly obtain morphological characteristics of the pea gravel. Six morphological parameters, including Elongation (E), Roundness (Round), Convexity Ratio (CR), Angularity Parameter (AP), Roughness (Rough) and Width were measured for each pea gravel sample. A sample size of 200 particles was randomly selected for each pea gravel sample to

ensure that the sample was large enough. Statistical analysis of aggregate morphological characteristics was performed to validate that the sample population is adequate, using Quantile-Quantile plot. If the data is normally distributed, the points in the QQ-normal plot line lie on a straight diagonal line. Tables 4 to 6 present the distributions of six morphological parameters for 10 pea gravel samples. The three tables show the ranges and the mean values of morphological characteristics for 10 pea gravel samples.

Table 4. Statistical results of the properties Elongation (E) and Roundness (Round)

Index	E				Round			
	Minimum	Maximum	Mean	Standard deviation	Minimum	Maximum	Mean	Standard deviation
S1	2.70	1.04	1.51	0.308	1.41	1.00	1.11	0.085
S2	3.74	1.05	1.56	0.442	1.93	1.05	1.29	0.138
S3	2.67	1.01	1.46	0.315	1.36	1.00	1.05	0.068
S4	2.60	1.02	1.43	0.280	1.36	1.00	1.05	0.060
S5	2.67	1.06	1.52	0.289	1.62	1.08	1.25	0.096
S6	3.28	1.01	1.55	0.377	1.77	1.07	1.26	0.128
S7	2.88	1.03	1.53	0.352	1.77	1.06	1.25	0.125
S8	2.88	1.03	1.53	0.352	1.85	1.06	1.27	0.115
S9	2.75	1.03	1.48	0.328	1.95	1.00	1.12	0.116
S10	1.91	1.03	1.37	0.196	1.18	1.00	1.04	0.048

Table 5. Statistical results of the properties Angularity Parameter (AP) and Convexity Ratio (CR)

Index	AP				CR			
	Minimum	Maximum	Mean	Standard deviation	Minimum	Maximum	Mean	Standard deviation
S1	1.13	0.87	0.98	0.046	1.437	1.089	1.203	0.0588
S2	1.20	0.93	1.02	0.048	1.371	1.072	1.203	0.0591
S3	1.06	0.81	0.93	0.045	1.435	1.069	1.183	0.0533
S4	1.03	0.90	0.96	0.021	1.342	1.044	1.156	0.0391
S5	1.12	0.93	1.00	0.037	1.387	1.101	1.198	0.0543
S6	1.11	0.88	0.98	0.042	1.519	1.079	1.206	0.0591
S7	1.13	0.87	0.98	0.040	1.387	1.103	1.209	0.0501
S8	1.08	0.86	0.97	0.044	1.338	1.072	1.198	0.0548
S9	1.14	0.88	0.99	0.044	1.444	1.056	1.216	0.0615
S10	1.03	0.91	0.96	0.022	1.266	1.086	1.154	0.0342

Table 6. Statistical results of the properties Roughness (Rough) and Width (W)

Index	Rough				W (mm)			
	Minimum	Maximum	Mean	Standard deviation	Minimum	Maximum	Mean	Standard deviation
S1	1.0807	0.9769	1.0289	0.02168	12.30	3.68	7.52	1.676
S2	1.097	0.989	1.0340	0.02080	12.74	4.51	8.23	1.796
S3	1.0953	0.9649	1.0287	0.03004	12.43	3.42	6.29	1.837
S4	1.05	0.9888	1.0214	0.01561	9.81	5.47	7.69	0.942
S5	1.0983	0.9899	1.0286	0.01997	9.98	4.98	7.18	1.030
S6	1.0971	0.9767	1.0273	0.02205	10.14	3.39	6.37	1.441
S7	1.0882	0.9828	1.0305	0.02333	10.41	3.06	6.64	1.612
S8	1.0971	0.9807	1.0310	0.02517	10.13	3.00	6.07	1.641
S9	1.0929	0.9823	1.0352	0.02608	10.72	3.81	6.89	1.402
S10	1.0495	0.9888	1.0194	0.01726	12.04	7.40	9.50	0.869

Table 7. Summary of morphological properties for the 10 pea gravel samples

Index	E	Round	AP	CR	Rough	W（mm）
S1	1.53	1.12	0.99	1.205	1.0284	8.03
S2	1.59	1.30	1.02	1.205	1.0336	8.76
S3	1.46	1.06	0.94	1.176	1.0265	7.22
S4	1.44	1.05	0.96	1.190	1.0210	7.81
S5	1.55	1.25	1.00	1.205	1.0278	7.38
S6	1.57	1.26	0.99	1.205	1.0279	6.84
S7	1.54	1.25	0.99	1.205	1.0294	7.24
S8	1.53	1.26	0.98	1.220	1.0307	6.73
S9	1.49	1.13	1.00	1.149	1.0344	7.31
S10	1.38	1.04	0.96	1.149	1.0194	9.61

Table 7 shows the values of the various morphological properties calculated by Equation 2 based on the obtained basic parameter information measured by the digital image processing. As it can be seen, for every property, differences exist among the 10 tested samples. As mentioned above, S4 and S5 are the same samples according to the sieve size. But when comparing the morphological characteristics of the two samples, each indicator provides a different degree of difference (see Table 7). These results reveal that the traditional sieving test results are the combined effect of various morphological characteristics. Even if the same sieving results have different particle properties, the morphological characteristics of the samples will be different.

Among the 6 obtained morphological properties (Table 7), the Elongation (*E*), Roundness (Round), Convexity Ratio (CR), and Angularity Parameter (AP) are indices used to describe the shape characteristic of the particles. The difference among the 4 indices is that E and Round focus on the shape, while CR and AP focus more on the outlines, which means that the elongated particles can either be angular or be rounded; the same is applicable for rounded particles. Therefore, in the present study, they are used as two different types of indicators, representing the shape and angular characteristics, respectively. With respect to the other two indices, the Roughness (Rough) is used to describe the surface texture, and Width (*W*) is used to describe the particle size.

Correlations between the morphological properties and the void content and the compressive strength of the MPS can be evaluated quantitatively. This will be analyzed and discussed in the following sections.

3.3. Compressive strength of the MPS

Table 8 shows the 28-day compressive strength test results of the hardened MPS made with 10 pea gravel samples described above. As can be seen, the test results vary from 5.89 MPa to 14.09 MPa, and the compressive strength of the MPS made with the river pebble is obviously smaller than that of the MPS made with the crushed rock.

Table 8. The 28-day compressive strength test results of the MPS made with the 10 pea gravel samples

ID	S1	S2	S3	S4	S5	S6	S7	S8	S9	S10
Compressive strength (MPa)	12.84	14.09	12.6	7.25	12.07	12.82	12.17	11.29	12.9	5.89

Test conducted by Jebli et al. [37] showed that the cement-aggregate interface is the weakest zone in concrete. In most of the investigations in literature, the parameters used for characterization of the interface are empirical [38, 39]. In the present study, the main reason for the difference between the two kinds of pea gravel materials is the surface texture of the particles. The photographs of the failure of the specimens made with the river pebble can help understand its effect on strength (see Fig. 6). This can be attributed to the fact that in the mixtures with river pebbles, the surface of the particles is smooth, resulting in a weak bond between the pebble and the slurry, and thus the mixtures have lower compressive strength than the mixtures with the crushed rocks. In addition, comparison of the compressive strength of the two mixtures made with the river pebbles shows that the compressive strength decreases as the particle size increases, which is contrary to the law of general concrete [40].

In the crushed rock samples, comparing the results among samples S2, S7 and S9, with the same undersize content, indicates that the compressive strength increases with the increase of oversize content.

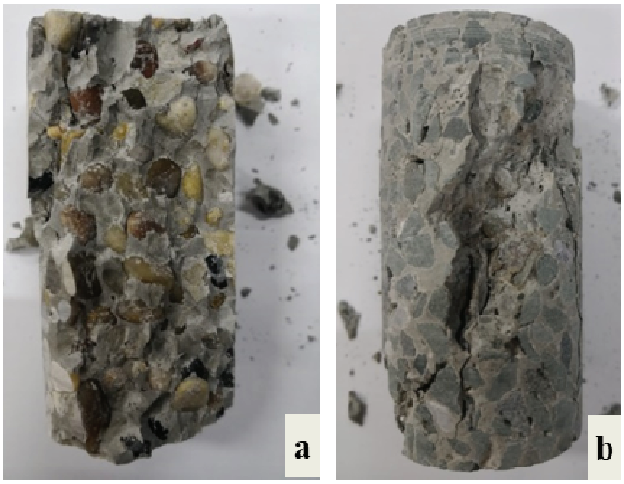

Fig. 6. Photos of failed specimens to show the difference between the MPS made with the river pebble and the crushed rock. a. Specimen made with the river pebble. b. Specimen made with the crushed rock

3.4. Relation between the void content and morphological properties

The values of the various morphological properties determined by the digital image processing are plotted against the void contents of the aggregate samples in Fig. 7. To show the overall trend of the correlation, the best-fitted straight lines are drawn on the graphs along with the plotted data points. As can be seen, the various morphological properties have different correlations with the void content.

Among the two shape factors (*E* and Roundness) measured, *E* is found to have a stronger correlation with the void content (the squared correlation coefficient, R^2 of 0.44) compared to that of the roundness (R^2 of 0.19). However, in absolute sense, the correlation of E to the void ratio is moderate and hardly any correlation exists between the void ratio and roundness. This result indicates that the change of the void content is only somewhat sensitive to Elongation.

Both the Convexity Ratio (CR), and Angularity Parameter (AP) are indices used to describe the angular characteristics of the particles. The R^2 values of their correlation to the void content are 0.48 and 0.46 (see Fig. 7c and 7d), respectively, which indicates that the angular characteristics of the particles have some impact on the porosity of the aggregate.

Surface texture factor (Rough) is really a measure of the roughness of the particle boundary. Fig. 7e shows the relation between the Roughness and void content. As can be seen, the increase of the roughness results in increasing void content, and the correlation degree (R^2 = 0.59) is higher than that for shape and angular factors. This result indicates that the surface texture of the particles plays an important role in the construction of the aggregate space skeleton.

Fig. 7f shows the correlation between the size factor (W) and the void content. Unlike other factors described above, the data of W plotted in Fig. 7f is highly scattered when all the tested data are combined. However, if the data of the river pebble is not considered, the size factor (W) and the void content have a very strong correlation. It can be seen that there is an excellent linear correlation (R^2 = 0.89) between W and the void content.

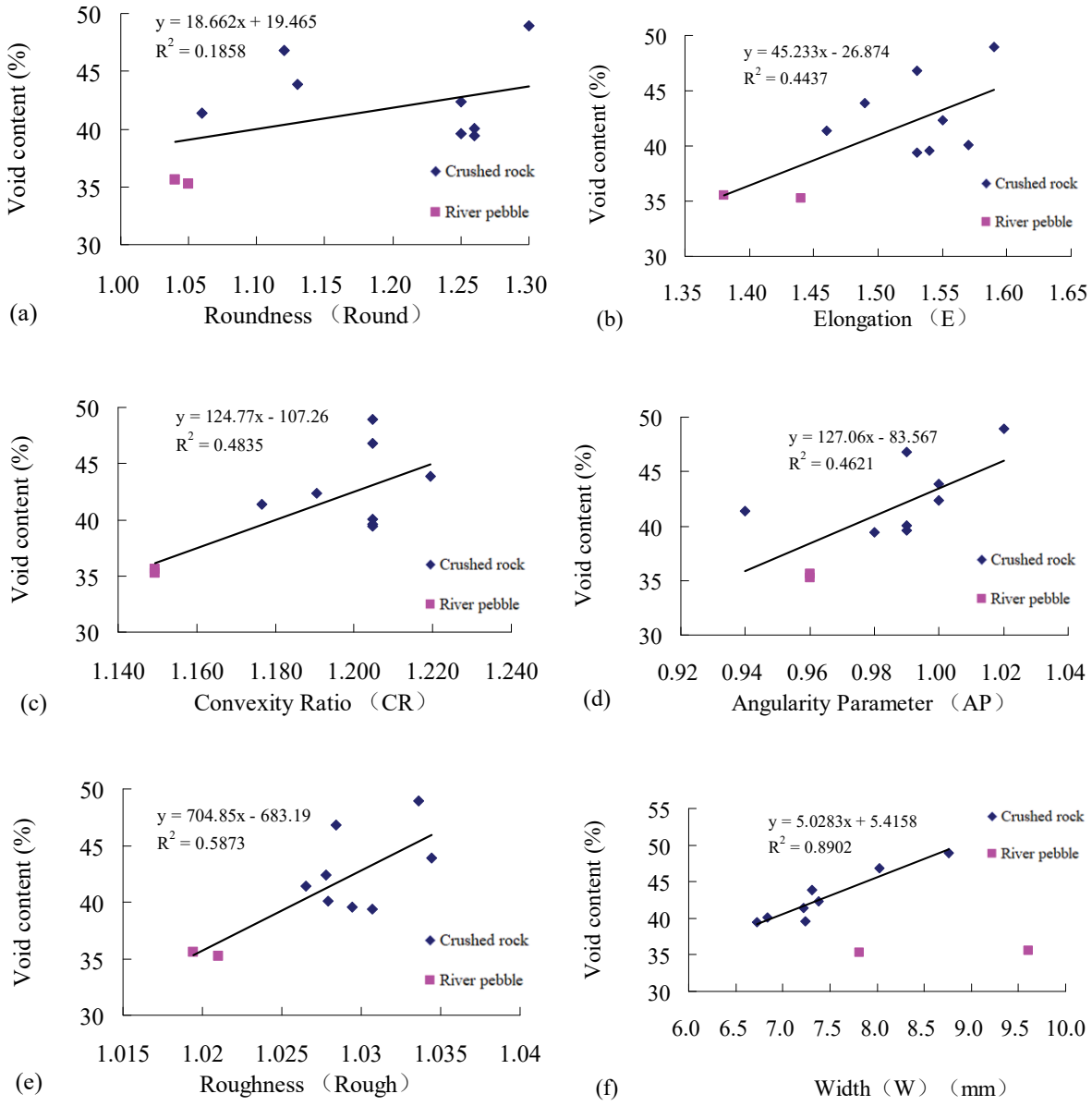

Fig. 7. Correlation of various morphological properties with the uncompacted void content

Since the void content is the result of the combined action of the various morphological properties, assuming that the relation between the morphological properties and void content can be expressed as a regression function, the factors of the shape, angularity, surface texture and the size of the particles were used along with the void ratio, to determine a relation between the morphological properties and void ratio using regression analysis. There is no obvious difference in the correlation between any one of the two angular factors (CR and AP) and the void content. Therefore, it is not necessary to include both the CR and AP in the regression equation. This led to obtaining two possible regression equations given below each having either CR or AP in the equation (Eqs. 3.1 and 3.2, respectively).

$$y = 2.34x_1 + 630.99x_2 + 23.43x_3 + 2.24x_4 - 662.69 \tag{3.1}$$

$$y = -91.91x_1 + 826.72x_2 + 45.96x_3 + 3.33x_4 - 813.01 \tag{3.2}$$

where: y is the void content, x_1 is the angular factor CR in Eq. 3.1 and is AP in Eq. 3.2, x_2 is the surface texture factor Roughness, x_3 is the shape factor E and x_4 is the size index W in mm.

When CR was used (Eq. 3.1), the correlation coefficient was $R = 0.88$ and the value of significance F was 0.07. When AP was used (Eq. 3.2), the correlation coefficient was $R = 0.90$ and the value of significance F was 0.04. These results indicate that the latter result is slightly better. Therefore, E, AP, Roughness and W can be used as typical indicators to describe the morphology of the pea gravel particles, and Eq. 3.2 can be used to roughly estimate the void content of the pea gravel aggregate with an acceptable accuracy.

3.5. Relation between the compressive strength and morphological properties

Fig. 8 shows the correlation of various morphological properties to compressive strength. As can be seen, morphological indices of E, CR and Roughness show moderately strong correlation to the compressive strength, which yields the values of R^2 of 0.65, 0.76 and 0.77, respectively (Fig. 8b, 8c, and 8e). On the other hand, the correlation of indices of Roundness and AP to the compressive strength is relatively weak. Also, for the size factor (W), there is a moderately strong linear correlation with $R^2 = 0.63$ for the crushed rock samples, as shown in Fig. 8f.

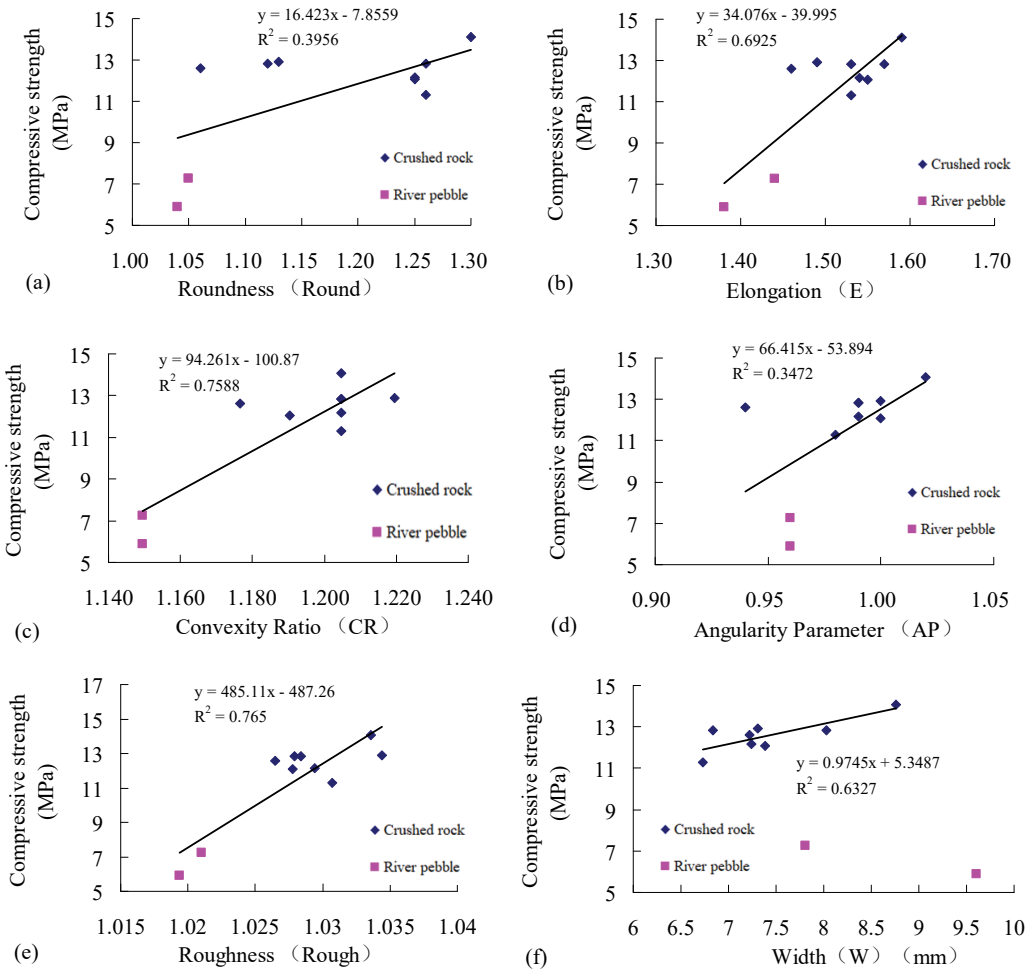

Fig. 8 Correlation of the various morphological properties to the compressive strength of the MPS made with different pea gravel samples

The above results may be compared with the analysis conclusions of the influencing factors for the void ratio. The comparison results show that the two conclusions are not too different. The roundness is weakly correlated to both the void ratio and strength. For single-size aggregates, the correlation between the void ratio and particle size is stronger than that between the particle size and strength; both correlations are quite strong. The effect of convexity and roughness on the strength is greater than that on the void ratio.

Also, it can be seen that there is noticeable difference in the correlation of the two angular factors (CR and AP) to the compressive strength and the void content.

Through the above analysis, it is shown that the extracted morphological indicators can reflect the characteristics of the pea gravel sample. Assuming that the relation between the morphological properties and the compressive strength can be expressed as a simple regression function, the factors of the shape, angularity, surface texture and the size of the particles were used along with

the compressive strength to determine a relation between the morphological properties and compressive strength using regression analysis. Among the morphological indicators, *E*, CR, Roughness and *W* were selected as representative parameters of morphological indicators to include in the first possible regression equation (Eq. 3.3). Considering the strong correlation that exists between the AP and the void content, a second possible equation was considered replacing CR by AP (Eq. 3.4). Based on the experimental data, the following two equations resulted from the regression analysis:

$$y = 8.49x_1 + 274.58x_2 + 14.90x_3 - 0.25x_4 - 301.50 \tag{3.3}$$

$$y = -67.11x_1 + 443.76x_2 + 31.80x_3 + 0.52x_4 - 430.71 \tag{3.4}$$

where: y is the compressive strength in MPa, x_1 is the angular factor CR in Eq. 3.3 and is AP in Eq. 3.4, x_2 is the surface texture factor Rough, x_3 is the shape factor E and x_4 is the size index W in mm.

When the CR was used (Eq. 3.3), the correlation coefficient was R = 0.84 and the value of significance F was 0.03. When the AP was used (Eq. 3.4), the correlation coefficient was R = 0.91 and the value of significance F was 0.008. These results indicate that the latter result is a little better. It is somewhat a surprise to see that the regression equation generated with AP is better than that generated with CR because the CR had a much stronger correlation with the compressive strength compared to that with AP. It is possible for this to happen because the data used were not fully independent and had interactions among the parameters. In other words, it was not possible to use data where only one parameter is changed at a time keeping the values of all other parameters constant. Due to the aforementioned results, both Eq. 3.3 and Eq.3.4 are recommended to predict the compressive strength of the MPS made with the pea gravel material.

4. Conclusions

The main purpose of the present study is to propose the quantitative morphological indices of pea gravels and establish their relations with the void content of the aggregate and the compressive strength of the MPS. Three types of experiments were carried out on 10 pea gravel samples, including artificial gravel and natural pebble, to obtain the morphological indices, the void content

and the compressive strength, respectively. Based on the experimental results of this study, the following conclusions can be drawn:

1. The research results show that with the help of digital image analysis, the quantitative indexes of the morphological characteristics of pea gravel can be obtained quickly and effectively, which provides a basis for the screening and quality control of pea gravel in TBM constructed project.
2. In the loose condition, the pea gravel of the crushed rock generally have a larger void content than that of the river pebble, and the grain size has the highest influence on the void ratio. The elongation, roughness and angularity have moderate influences on the void ratio. The content of the oversize or undersize particles in the sample affects the void ratio of the granular assembly in a contrary way.
3. The results of compressive strength show that the compressive strength of the MPS made with the river pebble is obviously smaller than that of the MPS made with the crushed rock. In the crushed rock samples, the compressive strength increases with the increase of the oversize particle content.
4. Relation between the morphological properties and the void content is expressed as a regression function including the following morphological properties: shape, angularity, surface texture and the size of the particles. This relation can be used to estimate the void content of the pea gravel aggregate with an acceptable accuracy.
5. Two regression relations between the compressive strength of the MPS and 4 morphological properties are proposed. These relations can be used for the prediction of the compressive strength of the MPS.
6. The outcomes of this study would assist with quality assessments in TBM engineering for the selection of the pea gravel material and the quality control of the MPS.

Acknowledgements:

This research was financed by the Research Foundation of SKLGP (No. SKLGP2016Z013). We express our gratitude to Pro. P.H.S.W. Kulatilake (Jiangxi University of Science and Technology, Ganzhou, China; Formerly at University of Arizona, Tucson, USA) for helping improving the structure and the language of the paper and advices about the interpretation of the data.

References

[1] EFNARC. Specification and guidelines for the use of specialist products for Mechanized Tunnelling (TBM) in Soft Ground and Hard Rock. www.efnarc.org. 2005.

[2] Maidl B., Herrenknecht M., Maidl U., Wehrmeyer G. Mechanised shield tunnelling / 2nd ed. Ernst & Sohn, 2011.

[3] Pelizza S., Peila D., Borio L., Dal Negro E., Schulkins R. and Boscaro A. Analysis of the Performance of Two Component Back-filling Grout in Tunnel Boring Machines Operating under Face Pressure. Proceedings of ITA-AITES World Tunnel Congress 2010: "Tunnel vision towards 2020", Vancouver, May (2010), pp. 14–20.

[4] Maidl O. I. H. C. M. B., Schmid L., Ritz W., et al. Hardrock Tunnel Boring Machines. Ernst & Sohn, 2008. https://doi.org/10.1002/9783433600122

[5] Peila D., Luca B., Sebastiano P. The behaviour of a two-component backfilling grout used in a tunnel-boring machine. Acta geotechnica Slovenica, 2011.

[6] Thewes M., Budach C. Grouting of the annular gap in shield tunnelling – an important factor for minimisation of settlements and production performance. Proceedings of the Ita, 2009.

[7] Henzinger M. R., Radončić N., Moritz B. A., et al. Backfill of segmental lining – State of the art, redistribution behaviour of pea gravel, possible improvements / Tübbingbettung – Stand der Technik, Umlagerungsverhalten von Perlkies, Verbesserungspotenzial. Geomechanik Und Tunnelbau. 9 (3): pp. 188–199, 2016.

[8] Lanaro F., Tolppanen P. 3D characterization of coarse aggregates. Engineering Geology. 65 (1): pp. 17–30, 2002. https://doi.org/10.1016/S0013-7952(01)00133-8

[9] Sengul Ö., Tasdemir C., Tasdemir M. A. Influence of aggregate type on mechanical behaviour of normal and high-strength concretes. ACI Mater J. 99 (6): pp. 528–533, 2002.

[10] Goble C. F., Cohen M. D. Influence of aggregate surface area on mechanical properties of mortar. ACI Mater J. 96 (6): pp. 657–662, 1999.

[11] Mehta P. K., Ezeldin A. S., Aitcin P. C. Effect of coarse aggregate on the behavior of normal and high-strength concretes. Cement Concrete and Aggregates. 13(2): p. 4, 1991. https://doi.org/10.1520/CCA10128J

[12] Cetin A., Carrasquillo R. L. High-performance concrete: influence of coarse aggregates on mechanical properties. ACI Mater J. 95 (3): pp. 252–261, 1998.

[13] Zhou F. P., Lydon F. D., Barr BIG. Effect of coarse aggregate on elastic modulus and compressive strength of high-performance concrete. Cem Concr Res. 25 (1): pp. 177–186, 1995. https://doi.org/10.1016/0008-8846(94)00125-I

[14] Uddin M. T., Mahmood A. H. Effects of maximum aggregate size on upv of brick aggregate concrete. Ultrasonics. 69: pp. 129–136, 2016. https://doi.org/10.1016/j.ultras.2016.04.006

[15] Kawamoto R., Andrade J., Matsushima T. A 3-D mechanics-based particle shape index for granular materials. Mechanics Research Communications. 92: 67–73, 2018. https://doi.org/10.1016/j.mechrescom.2018.07.002

[16] Wu J., Wang L., Hou Y., et al. A digital image analysis of gravel aggregate using CT scanning technique. International Journal of Pavement Research and Technology. 11 (2): pp. 160–167, 2018. https://doi.org/10.1016/j.ijprt.2017.08.002

[17] Nikbin I. M., Beygi M. H. A., Kazemi M. T., et al. A comprehensive investigation into the effect of aging and coarse aggregate size and volume on mechanical properties of self-compacting concrete. Materials & Design. 59: pp. 199–210, 2014. https://doi.org/10.1016/j.matdes.2014.02.054

[18] Masad E., Jandhyala V. K., Dasgupta N., Somadevan N., Shashidhar N. Characterization of air void distribution in asphalt mixes using X-ray computed tomography. J Mater Civil Eng. 14 (2): pp. 122–129, 2002. https://doi.org/10.1061/(ASCE)0899-1561(2002)14:2(122)

[19] Meddah M. S., Zitouni S., Belâabes S. Effect of content and particle size distribution of coarse aggregate on the compressive strength of concrete. Constr Build Mater. 24 (4): pp. 505–512, 2010. https://doi.org/10.1016/j.conbuildmat.2009.10.009

[20] Masad E., Button J. W. Unified imaging approach for measuring aggregate angularity and texture. Comput-Aided Civil Infrastruct Eng. 15: pp. 273–280, 2000. https://doi.org/10.1111/0885-9507.00191

[21] Caliskan S., Karihaloo B. L. Effect of surface roughness, type and size of model aggregates on the bond strength of aggregate/mortar interface. Interface Science. 12(4): pp. 361–374, 2004. https://doi.org/10.1023/B:INTS.0000042334.43266.62

[22] Zhang D., Huang X., Zhao Y. Investigation of the shape, size, angularity and surface texture properties of coarse aggregates. Constr Build Mater. 34: pp. 330–336, 2012. https://doi.org/10.1016/j.conbuildmat.2012.02.096

[23] Masad E., Muhunthan B., Shashidhar N., Harman T. Internal structure characterization of asphalt concrete using image analysis. Journal of Computing in Civil Engineering. 13 (2): pp. 88–95, 1999. https://doi.org/10.1061/(ASCE)0887-3801(1999)13:2(88)

[24] Mora C., Kwan A. Sphericity, shape factor, and convexity measurement of coarse aggregate for concrete using digital image processing. Cement & Concrete Research. 30 (3): pp. 351–358, 2000. https://doi.org/10.1016/S0008-8846(99)00259-8

[25] Roussillon T., Piégay H., Sivignon I., Tougne L., Lavigne F. Automatic computation of pebble roundness using digital imagery and discrete geometry. Comput. Geosci. 35: pp. 1992–2000, 2009. https://doi.org/10.1016/j.cageo.2009.01.013
[26] Al-Rousan T., Masad E., Tutumluer E., Pan T. Evaluation of image analysis techniques for quantifying aggregate shape characteristics. Constr Build Mater. 21 (5): pp. 978–990, 2007. https://doi.org/10.1016/j.conbuildmat.2006.03.005
[27] Rao C., Tutumluer E., Kim I. T. Quantification of coarse aggregate angularity based on image analysis. Transport Res Rec. 1787: pp. 117–124, 2002. https://doi.org/10.3141/1787-13
[28] Drevin G. R. Computational methods for the determination of roundness of sedimentary particles. Math. Geol. 38: pp. 871–890, 2007. https://doi.org/10.1007/s11004-006-9051-y
[29] Montenegro Ríos A., Sarocchi D., Nahmad-Molinari Y., Borselli L. Form from projected shadow (FFPS): an algorithm for 3D shape analysis of sedimentary particles. Comput. Geosci. 60: pp. 98–108, 2013. https://doi.org/10.1016/j.cageo.2013.07.008
[30] Hayakawa Y., Oguchi T. Evaluation of gravel sphericity and roundness based on surface-area measurement with a laser scanner. Comput. Geosci. 31: pp. 735–741, 2005. https://doi.org/10.1016/j.cageo.2005.01.004
[31] Lin C. L., Miller J. D. 3D characterization and analysis of particle shape using X-ray microtomography (XMT). Powder Technol. 154: pp. 61–69, 2005. https://doi.org/10.1016/j.powtec.2005.04.031
[32] Zhao B., Wang J. 3D quantitative shape analysis on form, roundness, and compactness with μCT. Powder Technol. 291: pp. 262–275, 2016. https://doi.org/10.1016/j.powtec.2015.12.029
[33] Mathieu C., Hervé, Piégay, Jérôme, Lavé, Lise V., Danang H. S., Sandy W. B., et al. Evaluating a 2d image-based computerized approach for measuring riverine pebble roundness. Geomorphology. 311: pp. 143–157, 2018. https://doi.org/10.1016/j.geomorph.2018.03.020
[34] Koohmishi M., Palassi M. Evaluation of morphological properties of railway ballast particles by image processing method. Transportation Geotechnics. 12: pp. 15–25, 2017. https://doi.org/10.1016/j.trgeo.2017.07.001
[35] Ding, X., Ma, T., Gao, W. Morphological characterization and mechanical analysis for coarse aggregate skeleton of asphalt mixture based on discrete-element modeling. Construction & Building Materials, 154 (Nov. 15): pp. 1048–1061, 2017. https://doi.org/10.1016/j.conbuildmat.2017.08.008
[36] Janoo, V. C., Bayer, J. J. The effect of aggregate angularity on base course performance. Effect of Aggregate Angularity on Base Course Performance. 2001.
[37] Jebli, M., Jamin, F., Malachanne, E., Garcia-Diaz, E., Youssoufi, M. E. Experimental characterization of mechanical properties of the cement-aggregate interface in concrete. Construction & Building Materials, 161 (Feb. 10): pp. 16–25, 2017. https://doi.org/10.1051/epjconf/201714012014
[38] Gu, X., Li, H., Wang, Z., Feng, L. Experimental study and application of mechanical properties for the interface between cobblestone aggregate and mortar in concrete – science direct. Construction and Building Materials, 46(46): pp. 156–166, 2013. https://doi.org/10.1016/j.conbuildmat.2013.04.028
[39] Koohmishi, M., Palassi, M. Evaluation of morphological properties of railway ballast particles by image processing method. Transportation Geotechnics. 12: pp. 15–25, 2017. https://doi.org/10.1016/j.trgeo.2017.07.001
[40] Siregar A. P. N., Rafiq M. I., Mulheron M. Experimental investigation of the effects of aggregate size distribution on the fracture behaviour of high strength concrete. Constr Build Mater. 150: pp. 252–259, 2017. https://doi.org/10.1016/j.conbuildmat.2017.05.142

Received: 2020-12-21, Revised: 2021-04-28